RSC Advances

PAPER

View Article Online
View Journal | View Issue

Cite this: *RSC Adv.*, 2019, **9**, 5417

Molecule design and properties of bridged 2,2-bi(1,3,4-oxadiazole) energetic derivatives

Xinghui Jin, *[a] Menghui Xiao,[a] Guowei Zhou,[a] Jianhua Zhou[a] and Bingcheng Hu[b]

Received 1st December 2018
Accepted 29th January 2019

DOI: 10.1039/c8ra09878f

rsc.li/rsc-advances

A series of bridged 2,2-bi(1,3,4-oxadiazole) energetic derivatives were designed and their geometrical structures, electronic structures, heats of formation, detonation properties, thermal stabilities and thermodynamic properties were fully investigated by density functional theory. The results showed that the $-N_3$ group and the –N– bridge play an important role in improving heats of formation of these 2,2-bi(1,3,4-oxadiazole) derivatives. The calculated detonation properties indicated that the $-NF_2$ group and the –N– bridge were very useful for enhancing the heats of detonation, detonation velocities and detonation pressures. Twenty-four compounds were found to possess equal or higher detonation properties than those of RDX, while 14 compounds had equal or higher detonation properties than those of HMX. The analysis of the bond-dissociation energies suggested that the –CN group was the effective structural unit for increasing the thermal stabilities while the $-NHNH_2$ group decreased these values. Overall, taking both the detonation properties and thermal stabilities into consideration, 22 compounds (A4, A6, A8, A9, B4, B9, C2, C3, C4, C5, C7, C, C9 D4, D8, D9, E9, F4, F9, G9, H4 and H9) were selected as the potential candidates for high-energy-density materials.

1. Introduction

Nitrogen-rich energetic materials with high densities, high positive heats of formation, excellent detonation properties (detonation velocity and detonation pressure) and acceptable thermal stabilities have gained considerable attention in the area of high-energy-density materials.[1–7] Five- or six-numbered heterocyclic compounds were found to be one of the most effective structural units for synthesizing high-energetic-density materials. Not surprisingly, 1,2,4-oxadiazole, 1,2,5-oxadiazole, 1,3,4-oxadiazole, and 1,2,3-oxadiazole, which are named as oxadiazoles, contain this type of structure with a nitrogen content of 40%. To the best of our knowledge, a large number of 1,2,4-oxadiazole and 1,2,5-oxadiazole (furazan)-based energetic materials are synthesized and their properties are fully investigated, while there has been fewer research on either 1,3,4-oxadiazole or 1,2,3-oxadiazole-based energetic materials.[8–11] Additionally, 1,2,3-oxadiazole is also presented as an unstable structure, which reverts to the diazoketone tautomer.[12] Consequently, 1,3,4-oxadiazole and their derivatives may offer good backbones for the development of new energetic compounds. Recently, a promising high-energy-density material based on 1,3,4-oxadiazole (Scheme 1, ICM-101) was synthesized with excellent detonation properties (ρ, 1.99 g cm^{-3}; D, 9481 m s^{-1} and P, 41.9 GPa) and thermal stabilities (T_d, 210 °C).[13] Then, it led to the idea of what changes will happen if other energetic groups and bridges were introduced to the bi-1,3,4-oxadiazole structure.

In this study, a systematic research on the heats of formation, electronic structures, detonation properties, thermal stabilities and thermodynamic properties of 1,3,4-oxadiazole bridged compounds (such as $-CH_2-$, –NH–, –O–, $-CH_2-CH_2-$, –CH=CH–, –NH–NH– and –N=N–) with various energetic groups (such as –CN, $-N_3$, $-NO_2$, $-NF_2$, $-NH_2$, $-NHNO_2$, $-NHNH_2$, $-CH(NO_2)_2$ and $-C(NO_2)_3$) (Scheme 2, series A–H) were reported.

2. Computational methods

The density functional theory (DFT) method has been demonstrated as an economical and liable tool in predicting the physicochemical properties of energetic materials. Studies on the optimized molecular structures, accurate energies, frontier molecular orbitals, heats of formation, vibrational frequencies, energetic properties, bond dissociation energies and thermodynamic parameters of the designed compounds were carried out by using the hybrid DFT/B3LYP functional with the 6-311G(d,p) basis set.[14,15] All the calculations were performed on the Gaussian 03 software[16] and the optimized structures were characterized to be the local energy minimum on the potential energy surface without imaginary frequencies.

Heat of formation (HOF) was an important parameter in evaluating the energetic properties of an energetic material.

[a]Key Laboratory of Fine Chemicals in Universities of Shandong, School of Chemistry and Pharmaceutical Engineering, Qilu University of Technology (Shandong Academy of Sciences), Ji'nan 250353, China. E-mail: jingetiema0000@126.com
[b]School of Chemical Engineering, Nanjing University of Science and Technology, Nanjing, 210094, China

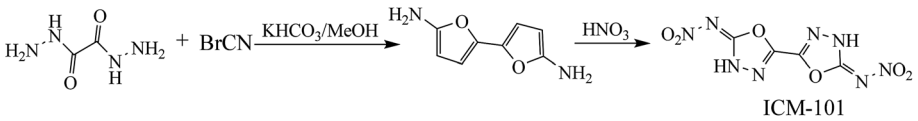

Scheme 1 Synthetic route of ICM-101.

Herein, isodesmic reactions were designed to predict the accurate gas-phase HOFs ($\Delta H_{f,gas}$) of the designed compounds. This is because, isodesmic reactions[17–21] can decrease the calculation errors of HOF greatly since all kinds of bonds and electronic environments of atoms in the reactants and products are very similar. The isodesmic reactions and related equations were presented in the following form (Scheme 3):

$$\Delta H_{298\ K} = \sum \Delta H_{f,p} - \sum \Delta H_{f,R} \quad (1)$$

$$\Delta H_{298\ K} = \Delta E_{298\ K} + \Delta(PV) = \Delta E_0 + \Delta ZPE + \Delta H_T + \Delta nRT \quad (2)$$

where $\Delta H_{298\ K}$ is the HOF that needs to be calculated, $\Delta H_{f,p}$ and $\Delta H_{f,R}$ are the HOFs of products and reactants, respectively, ΔE_0 is the energy change between products and reactants, ΔZPE is the difference between the zero-point energy (ZPE) of the products and reactants, ΔH_T is the thermal correction from 0 to 298 K, n is the number of energetic groups and $\Delta(PV)$ equals to ΔnRT.

Also, it should be noted that the HOFs of familiar species such as CH_4, CH_3NH_2, CH_3NHNH_2, CH_3NO_2, CH_3CN, CH_3CH_3, $CH_3CH_2CH_3$, CH_3NHCH_3 and $CH_3CH_2CH_2CH_3$ were available while the HOFs of CH_3NF_2, CH_3NHNO_2, CH_3N_3, $CH_3NHNHCH_3$, $CH_3N{=}NCH_3$, $CH_3CH(NO_2)_2$, $CH_3C(NO_2)_3$, and  were unavailable. Therefore, the atomization reaction $C_aH_bN_c \rightarrow aC(g) + bH(g) + cN(g)$ was employed to evaluate the HOFs of CH_3NF_2, CH_3NHNO_2, CH_3N_3, $CH_3NHNHCH_3$, $CH_3N{=}NCH_3$ and  at CBS-Q level[22] while the HOFs of the compounds $CH_3CH(NO_2)_2$ and $CH_3C(NO_2)_3$ were calculated *via* isodesmic reactions:

$$CH_3CH(NO_2)_2 + 2CH_4 \rightarrow CH_3CH_3 + 2CH_3NO_2$$

$$CH_3C(NO_2)_3 + 3CH_4 \rightarrow CH_3CH_3 + 3CH_3NO_2$$

Furthermore, HOFs of the energetic materials were always in the solid-phase, while HOFs that were obtained from the isodesmic reactions were in the gas-phase. According to Hess's law of constant heat summation, the values of $\Delta H_{f,gas}$ and heat of sublimation (ΔH_{sub}) can be used to evaluate the accurate data of solid-phase HOFs ($\Delta H_{f,solid}$) based on the following equation:[23]

$$\Delta H_{f,solid} = \Delta H_{f,gas} - \Delta H_{sub} \quad (3)$$

where, ΔH_{sub} is the heat of sublimation. Politzer *et al.* proposed that ΔH_{sub} can also be correlated with the molecular surface area A and the electrostatic interaction index $\nu\sigma_{tot}^2$ by the empirical expression:[24]

$$\Delta H_{sub} = aA^2 + b(\nu\sigma_{tot}^2)^{0.5} + c \quad (4)$$

where, a, b and c are coefficients and represented as 2.670×10^{-4} kcal mol^{-1} Å^{-4}, 1.650 kcal mol^{-1}, and 2.966 kcal mol^{-1}, respectively;[25] A is the surface area of the 0.001 e bohr^{-3} isosurface of electronic density of the molecule; ν is the degree of balance between positive and negative potential on the isosurface; σ_{tot}^2 is the measure of variability of the electrostatic potential on the molecular surface.

Densities (ρ) that were used to calculate the detonation velocity and detonation pressure were obtained by an improved equation proposed by Politzer *et al.*:[26]

$$\rho = \beta_1\left(\frac{M}{V}\right) + \beta_2\left(\nu\sigma_{tot}^2\right) + \beta_3 \quad (5)$$

where β_1, β_2, and β_3 are coefficients and represented as 0.9183, 0.0028, and 0.0443, respectively, M stands for the molecular mass (g mol^{-1}), V stands for the volume of a molecule (m^3 mol^{-1}), ν stands for the degree of balance between positive and negative potential on the isosurface and σ_{tot}^2 stands for measure of variability of the electrostatic potential on the molecular surface.

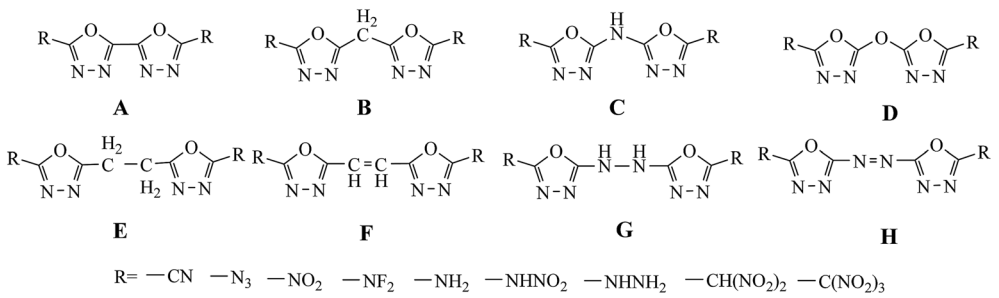

Scheme 2 The designed molecules based on bridged 2,2-bi(1,3,4-oxadiazole).

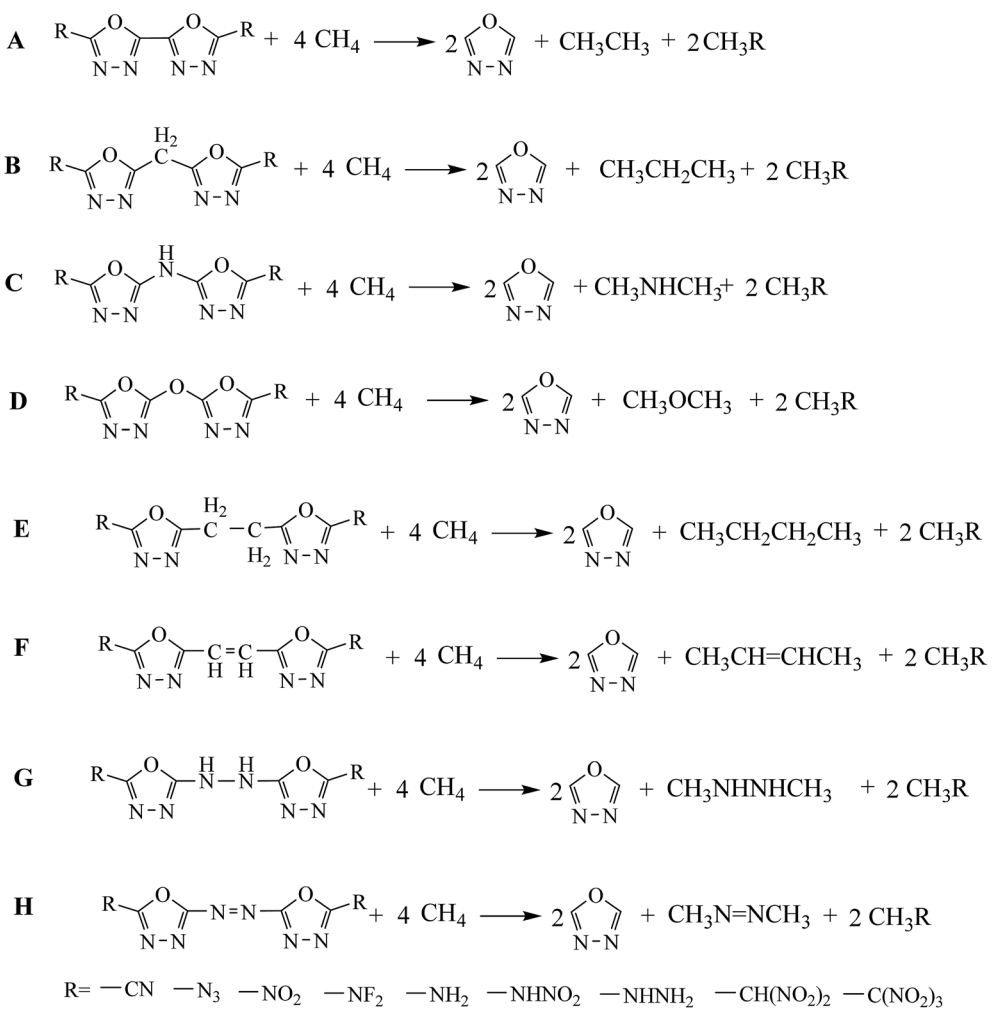

Scheme 3 The designed isodesmic reactions for each series of compounds.

Energetic properties (detonation velocity and detonation pressures) were estimated by the Kamlet–Jacobs equations:[27]

$$D = 1.01(N\bar{M}^{0.5}Q^{0.5})^{0.5}(1 + 1.3\rho) \quad (6)$$

$$P = 1.558\rho^2 N\bar{M}^{0.5}Q^{0.5} \quad (7)$$

where D is the detonation velocity (km s^{-1}); P is the detonation pressure (GPa); N, $\bar{M}$ and Q are the moles of detonation gases per-gram explosive (mol g^{-1}), the average molecular weight of these gases (g mol^{-1}) and heat of detonation (cal g^{-1}), respectively.

Bond dissociation energy (BDE), which is regarded as the strength of bonding, was an important indicator in predicting the way of bond cleavage and the thermal decomposition mechanism of high-energy-density materials. The homolytic BDEs were calculated as follows:

$$\mathrm{BDE}_0(A - B) = E_0(A^{\cdot}) + E_0(B^{\cdot}) - E_0(A - B) \quad (8)$$

The BDEs with zero-point energy (ZPE) corrections were finally calculated based on the following equation:

$$\mathrm{BDE}(A - B)_{\mathrm{ZPE}} = \mathrm{BDE}_0(A - B) + \Delta E_{\mathrm{ZPE}} \quad (9)$$

where ΔE_{ZPE} is the difference between the ZPEs of the products and the reactants.

3. Results and discussion

3.1 Electronic structures

The frontier molecular orbital which means the highest occupied molecular orbital (HOMO) and the lowest unoccupied molecular orbital (LUMO), can provide useful information on optical polarizability, kinetic stability and chemical reactivity.[28] The frontier molecular orbital energies and their energy gaps ($\Delta E_{\mathrm{LUMO-HOMO}}$) for the designed compounds are listed in Table 1. For each series, it is found that the HOMO energy levels increase evidently while the $-NH_2$ and $-NHNH_2$ groups are introduced to the rings. Oppositely, the HOMO energy levels decrease when attaching with other groups, especially the $-NF_2$ and $-C(NO_2)_3$ groups. The same is true for the LUMO energy levels. The influence of energetic groups on the sequence of the HOMO and LUMO energy levels can be written as follows: $-NH_2 \approx -NHNH_2 > -N_3 > -NHNO_2 > -NF_2 > -CN > -CH(NO_2)_2 > -NO_2$

Table 1 Calculated HOMO and LUMO energies (eV) and energy gaps ($\Delta E_{LUMO-HOMO}$) of the designed compounds

Compd	A1	A2	A3	A4	A5	A6	A7	A8	A9
HOMO	−8.76	−7.20	−9.25	−8.48	−6.26	−7.99	−6.24	−8.85	−9.18
LUMO	−3.85	−2.66	−4.41	−3.40	−1.52	−3.04	−1.65	−3.67	−4.24
$\Delta E_{HOMO-LUMO}$	4.91	4.54	4.84	5.08	4.74	4.95	4.59	5.18	4.94
Compd	B1	B2	B3	B4	B5	B6	B7	B8	B9
HOMO	−8.82	−7.45	−9.26	−8.61	−6.62	−8.19	−6.52	−8.93	−9.23
LUMO	−2.83	−2.06	−3.80	−2.29	−0.38	−2.60	−0.36	−3.44	−4.03
$\Delta E_{HOMO-LUMO}$	5.99	5.39	5.45	6.32	6.24	5.59	6.16	5.49	5.20
Compd	C1	C2	C3	C4	C5	C6	C7	C8	C9
HOMO	−7.85	−6.63	−8.19	−7.68	−5.93	−7.32	−6.00	−7.93	−8.25
LUMO	−2.88	−2.03	−3.82	−2.42	−0.20	−2.57	−0.44	−3.41	−4.04
$\Delta E_{HOMO-LUMO}$	4.97	4.60	4.37	5.26	5.73	4.75	5.56	4.52	4.21
Compd	D1	D2	D3	D4	D5	D6	D7	D8	D9
HOMO	−8.87	−7.52	−9.15	−8.67	−6.77	−8.28	−6.71	−8.96	−9.21
LUMO	−2.99	−2.28	−4.03	−2.56	−0.32	−2.68	−0.40	−3.51	−4.10
$\Delta E_{HOMO-LUMO}$	5.88	5.24	5.12	6.11	6.45	5.60	6.31	5.45	5.11
Compd	E1	E2	E3	E4	E5	E6	E7	E8	E9
HOMO	−8.68	−7.32	−9.05	−8.25	−6.47	−7.87	−6.53	−8.82	−9.14
LUMO	−2.75	−2.05	−3.66	−2.09	−0.01	−2.37	−0.40	−3.34	−3.96
$\Delta E_{HOMO-LUMO}$	5.93	5.15	5.39	6.16	6.46	5.50	6.13	5.48	5.18
Compd	F1	F2	F3	F4	F5	F6	F7	F8	F9
HOMO	−7.93	−6.73	−8.31	−7.73	−5.90	−7.36	−6.02	−7.99	−8.39
LUMO	−3.86	−2.96	−4.31	−3.59	−2.15	−3.26	−2.26	−3.79	−4.25
$\Delta E_{HOMO-LUMO}$	4.07	3.77	4.00	4.14	3.75	4.10	3.76	4.20	4.14
Compd	G1	G2	G3	G4	G5	G6	G7	G8	G9
HOMO	−7.40	−6.79	−7.66	−7.82	−5.81	−7.37	−6.16	−7.62	−8.26
LUMO	−2.55	−1.98	−3.61	−2.05	0.25	−2.35	−0.62	−3.36	−3.95
$\Delta E_{HOMO-LUMO}$	4.85	4.81	4.05	5.77	5.56	5.02	5.54	4.26	4.31
Compd	H1	H2	H3	H4	H5	H6	H7	H8	H9
HOMO	−8.52	−7.03	−9.02	−8.39	−6.29	−7.86	−6.21	−8.79	−9.09
LUMO	−4.97	−3.93	−5.25	−4.71	−3.11	−4.32	−3.17	−4.93	−5.22
$\Delta E_{HOMO-LUMO}$	3.55	3.10	3.77	3.68	3.18	3.54	3.04	3.86	3.87

≈ $-C(NO_2)_3$. Furthermore, the HOMO and LUMO energy levels present no regularity when different bridges are incorporated. The case is that, the LUMO energy levels decrease when –CH=CH– and –N=N– bridges are added, whereas the attaching of $-CH_2-$ and –O– bridges decreases the HOMO energy levels. Also, it should be noticed that the HOMO energy levels of series E ($-CH_2-CH_2-$ bridged ones) show no regularity compared with series A. Overall, incorporating different energetic groups and bridges into the rings shows different variation trends of HOMO and LUMO energy levels. It indicates that both the energetic groups and bridges interact with the frontier molecular orbitals.

Fig. 1 displays the variation trends of $\Delta E_{LUMO-HOMO}$ of the designed compounds. It is found that the volatilities of $\Delta E_{LUMO-HOMO}$ of series B, C, D, E and G are more evident than those of series A, F and H. It reveals that the parent structures are the main influence factors on $\Delta E_{LUMO-HOMO}$ for series A, F and H while the energetic groups make more contribution to $\Delta E_{LUMO-HOMO}$ for series B, C, D, E and G. The $\Delta E_{LUMO-HOMO}$ of the $-CH_2-$, –O– and $-CH_2-CH_2-$ bridged compounds increases, whereas the addition of –CH=CH– and –N=N– bridges decreases the $\Delta E_{LUMO-HOMO}$ evidently. But for the –NH– and –N=N– bridged compounds, there is less effect on $\Delta E_{LUMO-HOMO}$ compared with those of series A. Besides, the order of the average $\Delta E_{LUMO-HOMO}$ for each series can be written in the following form: $-CH_2-$ ≈ –O– ≈ $-CH_2-CH_2-$ > directly linked ≈ –NH– ≈ –NH–NH– > –CH=CH– > –N=N–. In view of all the designed compounds,

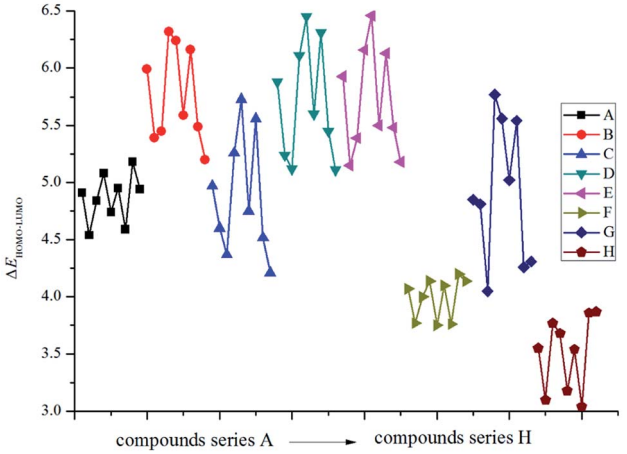

Fig. 1 The variation trends of $\Delta E_{LUMO-HOMO}$ of the designed compounds.

compound E5 (6.46 eV) has the highest $\Delta E_{LUMO-HOMO}$ while compound H7 (3.04 eV) has the smallest $\Delta E_{LUMO-HOMO}$. In other words, it is to say that compound H7 was the most reactive under external stimulus while compound E5 showed inertia to these stimuli.

3.2 Heats of formation

Heat of formation (HOF), which is usually taken as the indicator of the "energy content", is an important parameter in predicting the detonation properties (especially the heat of detonation) of an energetic material. Therefore, the accurate HOFs were predicted by either atomization reactions (mainly for small molecules) or isodesmic reactions (mainly for the title compounds). Table 2 lists the total energies, ZPEs, and thermal corrections for the reference compounds in the isodesmic reactions.

Table 3 presents the total energies, ZPEs, thermal corrections, $\Delta H_{f,gas}$, A, ν, σ_{tot}^2, ΔH_{sub} and $\Delta H_{f,solid}$ of the bridged 2,2-bi(1,3,4-oxadiazole) derivatives. It is seen that all the compounds (except for D5, −5.9 kJ mol^{-1}) have positive $\Delta H_{f,gas}$ in the range 28.6 (E5) to 2094.9 kJ mol^{-1} (C2). However, only 66 compounds (except for B5, −60.5 kJ mol^{-1}; D4, −23.9 kJ mol^{-1}; D5, −125.7 kJ mol^{-1}; E4, −18.8 kJ mol^{-1}; E5, −102.1 kJ mol^{-1}; F5, −5.0 kJ mol^{-1}) have positive $\Delta H_{f,solid}$ in the range 15.4 (E3) to 1970.6 kJ mol^{-1} (C2). It reveals that the –N_3 group plays an important role in improving the HOF of an energetic material while the –NH_2 group makes contribution to these data. Overall, the variation trends of the $\Delta H_{f,gas}$ and $\Delta H_{f,solid}$ were similar to each other. Again for $\Delta H_{f,solid}$, 60 compounds have higher $\Delta H_{f,solid}$ than that of RDX (79.0 kJ mol^{-1}) while 57 compounds have higher $\Delta H_{f,solid}$ than that of HMX (102.4 kJ mol^{-1}).[29] These high positive HOFs make a great contribution in increasing the detonation properties, such as heats of detonation, detonation velocities and detonation pressures.

Fig. 2 illustrates the variation trends in the $\Delta H_{f,solid}$ for the designed derivatives. It is found that the –NH– bridged compounds (series C) possess the highest $\Delta H_{f,solid}$ while the –CH_2–, –O–, –CH_2–CH_2–, –CH=CH–, –NH–NH– and –N=N– bridged ones have a lower $\Delta H_{f,solid}$. The influences of different bridge links on $\Delta H_{f,solid}$ can be written in the following order: –NH– > directly linked > –N=N– > –NH–NH– > –CH=CH– >

Table 2 Calculated total energies (E_0), zero-point energies (ZPE), thermal corrections (H_T) and heats of formation (HOFs) of the reference compounds

Compound.	E_0[a] (a.u.)	ZPE[a] (kJ mol^{-1})	H_T[a] (kJ mol^{-1})	$\Delta H_{f,gas}$ (kJ mol^{-1})
CH_4	−40.533748	117.0	10.0	−74.6[b]
CH_3NHNH_2	−151.217035	213.0	14.3	94.5[b]
CH_3NF_2	−294.298331	122.8	13.6	−98.4[c]
CH_3NH_2	−95.888444	167.6	11.4	−23.5[b]
CH_3NHNO_2	−300.434462	176.5	16.0	−8.5[c]
CH_3NO_2	−245.081687	130.6	13.9	−81.0[b]
CH_3CN	−132.793330	118.7	11.9	74.0[b]
CH_3N_3	−204.148401	131.7	14.2	289.9[c]
CH_3CH_3	−79.856261	195.3	11.6	84.0[b]
$CH_3CH_2CH_3$	−119.180686	270.4	14.4	−104.7[b]
CH_3NHCH_3	−135.695161	254.5	14.9	−19.0[b]
CH_3OCH_3	−155.071921	208.2	13.8	−184.1[b]
$CH_3CH_2CH_2CH_3$	−158.504982	345.1	17.7	−125.6[b]
$CH_3CH{=}CHCH_3$	−157.273161	282.0	16.9	−10.7[b]
$CH_3NHNHCH_3$	−190.535853	286.9	17.1	109.3[c]
$CH_3N{=}NCH_3$	−189.328011	220.6	16.0	160.5[c]
$CH_3CH(NO_2)_2$	−488.950712	212.3	22.8	81.8[d]
$CH_3C(NO_2)_3$	−693.479196	215.6	29.3	105.1[d]
	−262.161719	121.4	11.5	65.4[c]

[a] Calculated at B3LYP/6-311G(d,p) level. [b] Obtained from http://webbook.nist.gov. [c] Calculated values at the CBS-Q level. [d] Obtained by isodesmic reaction.

Table 3 Calculated total energies, thermal corrections, zero point energies, molecular properties and heats of formation of the designed compounds

Compd.	E_0 (au)	ZPE (kJ mol^{-1})	H_T (kJ mol^{-1})	$\Delta H_{f,gas}$ (kJ mol^{-1})	A (Å^2)	ν	$\sigma_{tot}{}^2$ (kcal mol^{-1})^2	ΔH_{sub} (kJ mol^{-1})	$\Delta H_{f,solid}$ (kJ mol^{-1})
A1	−707.621475	182.6	30.0	949.3	202.1	0.168	170.0	95.0	854.3
A2	−850.377196	207.6	34.6	1260.4	222.2	0.246	166.5	111.8	1148.6
A3	−932.180624	202.0	34.4	681.4	210.8	0.097	220.3	94.0	587.4
A4	−1030.617350	185.4	36.2	1032.6	207.1	0.204	170.3	101.1	931.5
A5	−633.893216	279.9	28.2	539.0	182.5	0.244	364.9	114.8	424.2
A6	−1042.926774	292.2	40.4	720.0	242.2	0.142	223.0	116.8	603.2
A7	−744.551016	370.9	35.3	774.8	214.3	0.250	254.4	118.8	656.0
A8	−1419.932522	362.7	55.9	696.2	304.2	0.076	247.5	145.8	550.4
A9	−1828.967187	366.7	70.1	800.0	344.7	0.076	145.0	168.1	631.9
B1	−746.957827	257.6	33.5	454.6	222.8	0.182	210.9	110.7	343.9
B2	−889.709693	282.9	38.1	776.0	244.1	0.240	175.7	123.9	652.1
B3	−971.519095	277.4	37.8	181.3	232.4	0.136	205.8	109.3	72.0
B4	−1069.953819	260.6	39.6	143.9	229.0	0.205	189.9	114.1	29.8
B5	−673.223066	355.4	31.6	61.6	204.5	0.250	332.5	122.1	−60.5
B6	−1082.261977	367.6	43.8	228.5	262.8	0.176	288.9	138.9	89.6
B7	−783.879076	446.3	38.6	302.0	234.9	0.240	240.9	126.6	175.4
B8	−1459.268527	437.9	59.3	477.8	324.4	0.108	250.4	166.0	311.8
B9	−1868.305088	442.0	73.6	576.8	365.0	0.091	201.7	190.9	385.9
C1	−763.000285	227.4	33.3	1764.4	216.3	0.149	278.6	109.2	1655.2
C2	−905.748663	252.0	38.3	2094.9	236.6	0.250	203.7	124.3	1970.6
C3	−987.561813	247.2	37.6	1490.6	225.0	0.109	277.3	107.0	1383.6
C4	−1085.994461	229.8	39.7	1458.4	221.8	0.154	249.4	110.2	1348.2
C5	−689.259280	324.7	31.8	1387.9	197.3	0.249	355.9	120.9	1267.0
C6	−1098.302817	336.8	43.8	1542.3	256.7	0.155	255.0	129.5	1412.8
C7	−799.916632	415.8	38.6	1624.7	229.0	0.250	266.0	127.4	1497.3
C8	−1475.310251	407.4	59.2	1789.5	318.4	0.083	306.7	160.6	1628.9
C9	−1884.348017	411.8	73.4	1885.6	358.5	0.062	259.1	183.7	1701.9
D1	−782.845020	194.3	32.4	384.1	213.3	0.190	153.3	100.5	283.6
D2	−925.594326	218.5	37.2	711.4	233.8	0.249	182.6	120.1	591.3
D3	−1007.399335	212.5	34.8	125.7	221.7	0.092	249.5	100.4	25.3
D4	−1105.836802	196.4	38.7	83.9	218.7	0.214	172.3	107.8	−23.9
D5	−709.108853	291.0	30.8	−5.9	194.4	0.239	372.2	119.8	−125.7
D6	−1118.150451	303.9	42.8	154.4	253.5	0.142	222.8	123.1	31.3
D7	−819.769222	383.1	37.5	224.0	225.6	0.250	252.1	124.1	99.9
D8	−1495.155645	374.4	58.3	407.5	315.1	0.089	235.1	155.0	252.5
D9	−1904.190918	378.5	72.6	509.9	355.6	0.084	145.9	177.9	332.0
E1	−786.288860	332.9	37.2	416.9	245.0	0.212	167.6	120.7	296.2
E2	−929.038343	357.7	41.8	744.2	264.9	0.224	182.2	135.0	609.2
E3	−1010.852874	351.7	41.8	135.8	250.7	0.177	169.0	120.4	15.4
E4	−1109.283300	335.3	43.0	109.5	245.8	0.237	206.7	128.3	−18.8
E5	−712.552050	429.5	35.7	28.6	223.0	0.249	331.5	130.7	−102.1
E6	−1121.592652	443.2	47.0	191.7	280.4	0.210	187.9	143.7	48.0
E7	−823.207464	521.2	42.2	270.8	257.4	0.238	243.9	139.1	131.7
E8	−1498.598700	513.1	63.0	442.4	346.9	0.122	217.1	182.5	259.9
E9	−1907.638388	517.0	77.3	533.0	385.7	0.108	167.6	208.1	324.9
F1	−785.062414	270.8	35.7	518.0	237.2	0.227	133.6	113.3	404.7
F2	−927.813680	295.5	40.4	840.6	257.4	0.228	155.9	127.6	713.0
F3	−1009.623916	290.6	40.0	244.2	245.8	0.172	157.0	115.8	128.4
F4	−1108.057319	273.1	42.1	209.9	242.3	0.237	133.4	116.9	93.0
F5	−711.326903	368.0	34.0	126.7	218.0	0.248	370.2	131.7	−5.0
F6	−1120.366353	380.8	46.0	292.6	277.3	0.188	180.2	138.6	154.0
F7	−821.987326	459.1	40.8	355.5	249.7	0.249	279.0	139.7	215.8
F8	−1497.372134	450.8	61.7	543.8	339.3	0.119	193.3	174.2	369.6
F9	−1906.410426	455.4	75.7	638.4	379.6	0.109	150.0	201.4	437.0
G1	−818.332921	270.6	34.4	610.8	232.2	0.171	229.6	116.0	494.8
G2	−961.083454	297.4	40.9	939.3	253.1	0.250	268.8	140.6	798.7
G3	−1042.894775	290.0	38.8	335.9	240.5	0.128	252.2	116.3	219.6
G4	−1141.330500	274.0	42.8	298.9	236.3	0.176	295.6	124.6	174.3
G5	−744.588899	368.9	32.5	242.8	213.1	0.250	323.7	125.3	117.5
G6	−1153.639466	381.7	46.8	381.8	271.1	0.172	255.1	140.3	241.5
G7	−855.244403	460.9	38.8	484.9	247.2	0.250	261.3	136.5	348.4
G8	−1530.635854	451.5	60.0	655.0	335.8	0.086	292.8	173.1	481.9

Table 3 (*Contd.*)

Compd.	E_0 (au)	ZPE (kJ mol^{-1})	H_T (kJ mol^{-1})	$\Delta H_{f,gas}$ (kJ mol^{-1})	A (Å^2)	ν	$\sigma_{tot}{}^2$ (kcal mol^{-1})^2	ΔH_{sub} (kJ mol^{-1})	$\Delta H_{f,solid}$ (kJ mol^{-1})
G9	−1939.685922	456.4	76.5	721.5	375.0	0.078	286.2	202.2	519.3
H1	−817.087030	205.7	35.1	765.1	228.9	0.190	158.8	108.9	656.2
H2	−959.828694	230.7	39.2	1112.7	244.6	0.250	148.6	121.4	991.3
H3	−1041.650351	225.8	39.0	486.5	237.3	0.114	212.8	109.4	377.1
H4	−1140.085203	130.6	13.9	343.5	233.6	0.230	178.8	117.7	225.8
H5	−743.369994	303.6	32.8	325.5	208.5	0.235	386.2	126.8	198.7
H6	−1152.393136	315.4	45.4	533.7	268.8	0.170	222.8	135.7	398.0
H7	−854.028806	393.8	40.4	558.4	240.4	0.249	262.2	132.8	425.6
H8	−1529.401790	386.8	60.2	777.9	330.5	0.088	246.4	166.7	611.2
H9	−1938.436395	390.6	74.7	882.0	371.2	0.094	148.9	192.3	689.7

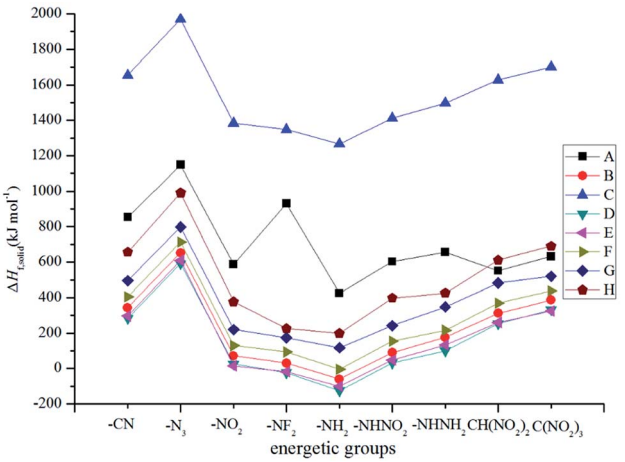

Fig. 2 The variation trends of $\Delta H_{f,solid}$ of the designed compounds.

–CH_2– > –CH_2–CH_2– > –O–. Obviously, the –NH– bridge is the most effective link in improving the $\Delta H_{f,solid}$ for the 2, 2-bi(1,3,4-oxadiazole) derivatives while the –O– bridge link has the opposite effect. The substituted derivatives with the conjugated bridges (–CH=CH– or –N=N–) have higher $\Delta H_{f,solid}$ than those of the corresponding ones with the unconjugated bridges (–CH_2–CH_2– or –NH–NH–). This may be caused by the large conjugated system that is built by 2,2-bi(1,3,4-oxadiazole) and the conjugated bridge. For each of the series, $\Delta H_{f,solid}$ increases evidently when the parent molecules are substituted by the –N_3 group, whereas the opposite is true for the –NH_2 substituent. The influences of the different energetic groups on $\Delta H_{f,solid}$ can be written in the following order for series B–H: –N_3 > –$C(NO_2)_3$ > –CN ≈ –$CH(NO_2)_2$ > –$NHNH_2$ > –$NHNO_2$ ≈ –NO_2 > –NF_2 > –NH_2 while that for series A can be presented as follows: –N_3 > –NF_2 > –CN > –$NHNH_2$ > –$C(NO_2)_3$ > –$NHNO_2$ ≈ –NO_2 > –$CH(NO_2)_2$ > –NH_2. Overall, all the results reveal that the effects of the bridged links on the $\Delta H_{f,solid}$ values of the designed compounds were coupled to those of the substituted energetic groups.

3.3 Detonation properties

The detonation properties that are related to oxygen balance (OB), density (ρ), heat of detonation (Q), detonation velocity (D) and detonation pressure (P) are summarized in Table 4. For a comparison, the detonation properties of the two well-known explosives 1,3,5-trinitro-1,3,5-triazinane (RDX) and 1,3,5, 7-tetranitro-1,3,5,7-tetrazocane (HMX) are also presented. It is seen that most of the designed compounds have a negative OB except for compounds A9, C9, D9, G9 and H9. Twenty-one compounds have higher OBs than those of RDX and HMX (−21.6%) while 51 compounds are on the opposite side. Generally speaking, it is better to keep the values of OB at around zero when designing energetic materials since too much oxygen will produce O_2, which will remove a great deal of the energy produced during the explosion process. Obviously, compounds A9 (7.34%), B9 (−3.56%), C9 (5.32%), D3 (−6.56%), D8 (−8.84%), D9 (10.62%), E9 (−13.79%), F9 (−10.39%), G9 (3.43%) and H9 (6.90%) possess acceptable values of OB. It can be deduced that –$C(NO_2)_3$ is the best group in controlling the OB of all the designed compounds while the –NO_2 and –$CH(NO_2)_2$ groups can only play an important role in controlling the OB of the –O– bridged compounds. The bridged 2,2-bi(1,3,4-oxadiazole) derivatives with different substituent groups are also found to have different ρ, Q, D and P values: values of ρ range from 1.54 (E5) to 2.16 g cm^{-3} (D4); values of Q range from 465.3 (E5) to 2586.9 cal g^{-1} (C4); values of D range from 5.46 (E5) to 10.6 km s^{-1} (A4) and values of P range from 12.0 (E5) to 54.5 GPa (A4). Interestingly, it is found that compound E5 has the smallest values of ρ, Q, D and P while compound A4 possesses the highest values of D and P. For a comparison, 28 compounds (A3, A4, A6, A9, B4, B9, C2, C3, C4, C6, C8, C9, D2, D3, D4, D6, D8, D9, E4, E9, F4, F9, G4, G6,G9, H4, H6 and H9) were found to have superior densities to that of RDX while 9 compounds (A4, A9, B4, C4, D4, D9, E4, F4, G4 and H4) were found to have superior densities to that of HMX; 24 compounds (A4, A6, A8, A9, B4, B9, C2, C3, C4, C5, C6, C7, C8, C9, D4, D8, D9, E9, F4, F9, G4, G9, H4 and H9) were found to possess equal or higher detonation velocities and detonation pressures than those of RDX while 14 (A4, A9, B9, C2, C3, C4, C6, C8, C9, D4, D8, D9, G4 and H4) compounds have equal or higher detonation velocities and detonation pressures than those of HMX.

Fig. 3 displays the variation trends of ρ, Q, D and P of the designed compounds together with those for the popular

Table 4 Predicted densities (ρ), heats of detonation (Q), detonation velocities (D) and detonation pressures (P) of the designed compounds

Compound	OB	ρ (g cm^{-3})	Q (cal g^{-1})	D (km s^{-1})	P (GPa)
A1	−85.11	1.64	1586.3	6.92	20.1
A2	−43.64	1.80	1675.3	8.38	31.2
A3	−38.10	1.83	1955.3	8.58	33.0
A4	−40.00	2.12	2311.0	10.60	54.5
A5	−76.19	1.68	1291.6	7.36	23.0
A6	−18.60	1.83	1694.1	8.88	35.3
A7	−72.73	1.69	1375.7	7.96	27.0
A8	−13.87	1.80	1770.4	8.79	34.3
A9	7.34	1.93	1640.7	9.19	39.0
B1	−102.97	1.58	925.8	5.82	13.8
B2	−61.54	1.72	1114.0	7.22	22.5
B3	−33.06	1.77	1281.5	7.81	26.8
B4	−56.69	2.00	1377.8	8.78	36.3
B5	−96.70	1.67	555.7	6.00	15.2
B6	−35.29	1.78	1195.3	7.86	27.3
B7	−90.57	1.63	743.0	6.67	18.6
B8	−26.67	1.78	1573.1	8.38	30.9
B9	−3.56	1.90	1691.9	9.15	38.3
C1	−82.76	1.64	2438.6	7.92	26.3
C2	−44.26	1.83	2427.3	9.42	39.8
C3	−16.46	1.84	2544.1	9.78	43.0
C4	−40.78	2.03	2586.9	10.58	53.8
C5	−74.32	1.71	2286.4	8.88	33.9
C6	−20.51	1.83	2329.6	9.69	42.0
C7	−71.36	1.73	2222.8	9.31	37.5
C8	−15.51	1.81	2425.8	9.61	41.1
C9	5.32	1.89	2217.2	9.83	44.1
D1	−70.59	1.69	1023.8	6.52	18.1
D2	−33.90	1.85	1196.6	7.97	28.6
D3	−6.56	1.85	1373.9	8.41	31.9
D4	−31.25	2.16	1458.5	9.67	45.8
D5	−60.87	1.73	720.6	6.63	19.0
D6	−11.68	1.85	1268.0	8.39	31.7
D7	−59.81	1.71	921.9	7.16	22.0
D8	−8.84	1.83	1885.2	9.17	37.7
D9	10.62	1.93	1424.0	9.42	41.0
E1	−118.52	1.55	862.9	5.56	12.3
E2	−77.42	1.63	1053.2	6.75	19.0
E3	−50.00	1.74	1200.7	7.49	24.4
E4	−71.64	1.95	1302.6	8.37	32.6
E5	−114.29	1.54	465.3	5.46	12.0
E6	−50.35	1.75	1139.7	7.57	25.0
E7	−106.19	1.55	650.8	6.24	15.7
E8	−38.50	1.72	1509.9	8.02	27.8
E9	−13.79	1.83	1632.7	8.76	34.2
F1	−112.15	1.58	941.8	5.68	13.2
F2	−71.54	1.66	1118.8	6.88	20.0
F3	−44.09	1.73	1274.1	7.50	24.3
F4	−66.17	2.03	1372.4	8.70	35.7
F5	−107.22	1.57	589.7	5.65	13.0
F6	−45.07	1.78	1199.0	7.70	26.2
F7	−100.00	1.57	746.3	6.33	16.3
F8	−34.41	1.74	1559.5	8.10	28.5
F9	−10.39	1.87	1674.4	8.90	36.0
G1	−80.73	1.67	1023.3	6.60	18.4
G2	−44.80	1.79	1182.9	7.83	27.1
G3	−18.60	1.84	1338.8	8.40	31.7
G4	−41.48	2.00	1424.0	9.14	39.3
G5	−72.73	1.69	725.7	6.78	19.6
G6	−22.22	1.82	1254.9	8.32	30.9
G7	−70.18	1.79	872.2	7.67	26.0

explosives RDX and HMX. Obviously, the variation trends of ρ, Q, D and P were approximately the same throughout the series. That is to say, the energetic molecules with higher ρ and Q will also possess higher D and P. It can be predicted that ρ and Q (or HOFs) are always the important factors to be considered when an energetic molecule is designed. Fig. 3(a) shows the influence of different energetic groups on density. It can be seen that the compounds that are substituted by the –NF_2 group have the highest ρ while the –CN, –NH_2 or –$NHNH_2$ substituted ones have a smaller ρ. When the bridge groups are –CH_2–, –CH_2–CH_2– and –CH=CH–, the ρ values of the designed compounds are smaller than those of the directly linked ones (series A) with the same substituents. In addition, compounds with the conjugated bridge –CH=CH– are found to have higher ρ than the corresponding ones with the unconjugated bridge –CH_2–CH_2–. Oppositely, compounds with the conjugated bridge –N=N– show no regularity compared to the corresponding ones with the unconjugated bridge –NH–NH–. Overall, the effects of the bridges on the ρ values are coupled to those of the substituents. Fig. 3(b) shows the influence of different energetic groups on Q. It is clearly seen that different bridge groups have different effects on Q values: the –NH– bridged compounds possess higher Q values than those of the other series with the same substituents, but the –CH_2–CH_2– bridged ones have the smallest values of Q compared to those of the other series with the same substituents. It can be inferred that the –NH– bridge is the most effective group in improving Q of the 2,2-bi(1,3,4-oxadiazole) derivatives while the –CH_2–CH_2– bridge will decrease the Q values. For a comparison, all the –NH– bridged compounds have higher Q values than those of RDX and HMX while Q values of the –O–, –CH_2–CH_2–, –CH=CH–, –NH–NH– and –N=N– bridged ones are smaller (except for D8, F9 and H8) than those of HMX. However, the Q values of the directly linked compounds (series A) fluctuated around Q values of RDX and HMX. Additionally, the –NH_2 substituted compounds were also found have the smallest values for all the designed compounds except for compound C7. It is predicted that the –NH_2 and –NHH_2 groups may make less contribution to the values of Q than other energetic groups. In view of Fig. 3(c) and (d), it is seen that the influence of the different energetic groups on the values of D and P is approximately the same throughout all the series. The general influence order of the different energetic groups on the values of D and P can be written as follows: –NF_2 > –$C(N_2)_3$ > –NO_2 ≈ –$NHNO_2$ ≈ –$CH(NO_2)_2$ > –N_3 ≈ –$NHNH_2$ > –NH_2 > –CN, while the influence of the different bridges on the values of D and P can be written in the order of –NH– > directly linked > –O– ≈ –NH–NH– ≈ –N=N– > –CH_2– > –CH_2–CH_2– ≈ –CH=CH–. It can be concluded that the –NF_2 and –NH– bridge are the most effective groups in improving the D and P values while it is on the opposite side for the –CN, –CH_2–CH_2– and –CH=CH– bridged compounds. It is also found that the compounds with the conjugated bridge have similar D and P values compared to the corresponding unconjugated bridged compounds. For example, the –CH_2–CH_2– bridged compounds have similar D and P values to that of the –CH=CH– bridged compounds, and the same is true of the –N=N– and –NH–NH– bridged ones. For a comparison, most of the –CN, –NH_2 or

Table 4 (*Contd.*)

Compound	OB	ρ (g cm^{-3})	Q (cal g^{-1})	D (km s^{-1})	P (GPa)
G8	−17.02	1.80	1614.3	8.70	33.6
G9	3.43	1.88	1601.3	9.08	37.5
H1	−74.07	1.65	1161.5	6.68	18.7
H2	−38.71	1.80	1334.6	8.04	28.6
H3	−12.50	1.82	1454.2	8.44	31.8
H4	−35.82	2.13	1440.4	9.52	44.2
H5	−65.31	1.70	832.1	6.79	19.8
H6	−16.78	1.85	1356.8	8.53	32.8
H7	−63.72	1.70	961.6	7.38	23.3
H8	−12.83	1.80	1676.7	8.73	33.8
H9	6.90	1.86	1571.4	8.89	35.8
RDX[30]	−21.6	1.82	1590.7	8.75	34.0
HMX[30]	−21.6	1.91	1633.9	9.10	39.0

–$NHNH_2$ substituted compounds have smaller D and P values than that of RDX. It is also worth noting that the –NH_2 or –$NHNH_2$ substituted compounds with the –NH– bridge have equal D and P values to those of RDX, and, consequently, the –NH– bridge is the most important influence group in improving D and P values rather than the energetic groups.

3.4 Thermal stabilities

The bond dissociation energy (BDE) for each of the possible trigger bonds was often investigated since it is an important factor in understanding the thermally stability, guaranteeing the safety and enhancing the controllability of kinetic energy release. Generally speaking, the smaller is the energy needed for breaking a bond, the weaker is the bond, and, consequently, this chemical bond may act as the trigger bond. Previous studies have also demonstrated that the bridge or energetic groups that are attached to the side chain of a ring usually act as the initial step during the decomposition process, and, thus, some possible trigger bonds were elucidated to predict the pyrolysis mechanism of the bridged 2,2-bi(1,3,4-oxadiazole) derivatives: (1) ring–R; (2) C–C (bridge); (3) C–N (bridge); (4) C–O (bridge); (5) N–N or N=N (bridge); (6) NH–NH_2 or NH–NO_2 or C–NO_2. Note that the possible trigger bonds with the weakest BDEs were selected as the breaking bonds based on natural bond orbital (NBO) analyses. Take compound G6 for example, the possible trigger bonds were C(ring)–$NHNO_2$, –C(ring)–N(bridge)–, –N–N–(bridge) and NH–NO_2, and the corresponding BDEs of these possible trigger bonds were 453.4, 357.6, 120.7 and 69.9 kJ mol^{-1}, respectively. Finally, the NH–NO_2 bond was selected as the trigger bond since it had the smallest value of

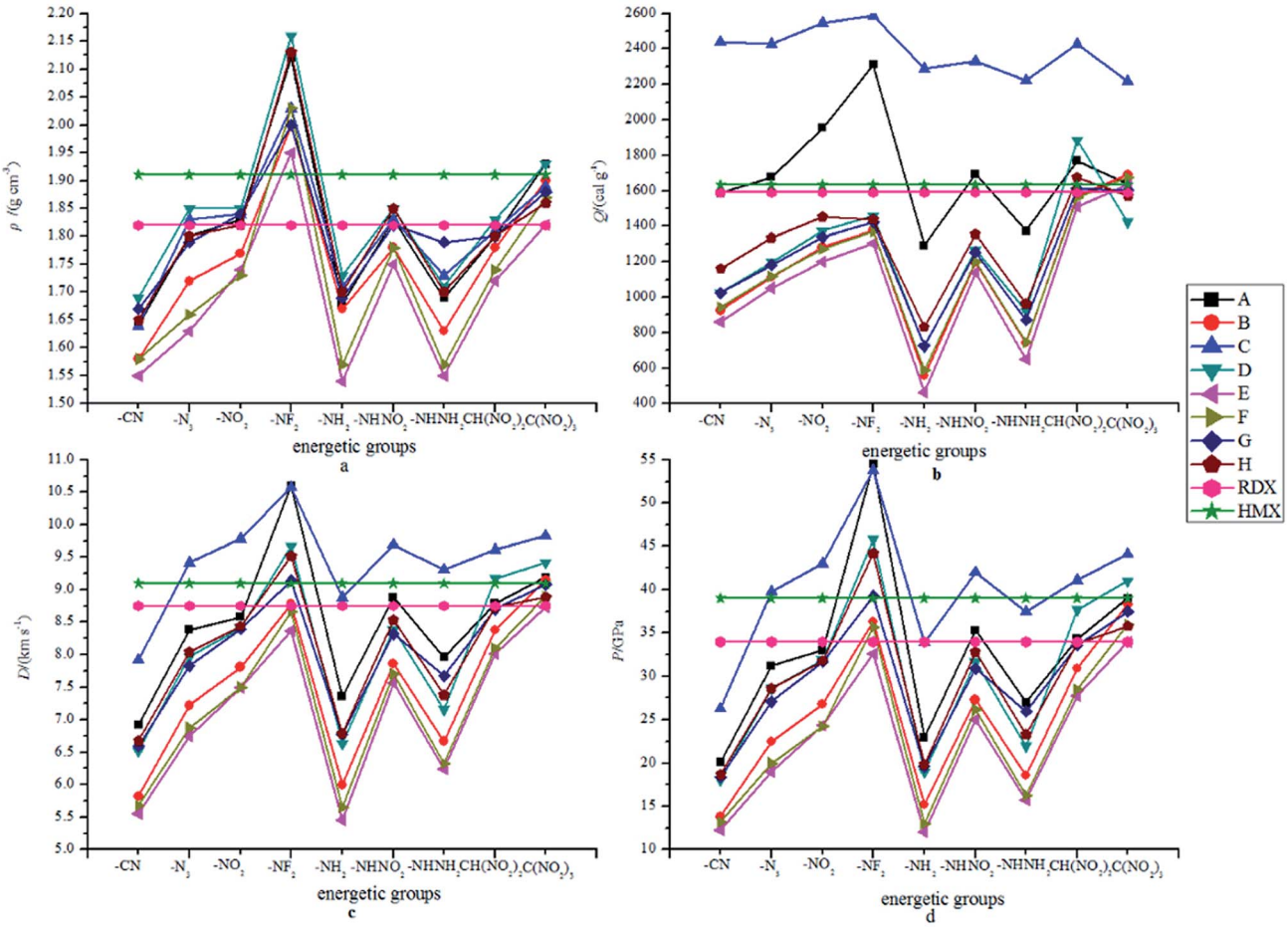

Fig. 3 The variation trends of ρ, Q, D and P of the designed compounds.

Table 5 Bond dissociation energies (BDE, kJ mol^{-1}) for the weakest bonds of the designed compounds

	Ring-R		C–C (bridge)		C–N (bridge)		C–O (bridge)		N–N/N=N (bridge)		NH–NH_2/NH–NO_2/C–NO_2	
Compd.	BO	BDE	BO	BDE	BO	BDE	BO	BDE	BO	BDE	BO	BDE
A1	1.082	551.0	1.063	522.8	—	—	—	—	—	—	—	—
A2	1.113	379.7	1.074	538.0	—	—	—	—	—	—	—	—
A3	0.893	245.8	1.062	489.1	—	—	—	—	—	—	—	—
A4	1.022	274.2	1.063	527.0	—	—	—	—	—	—	—	—
A5	1.169	476.8	1.078	534.4	—	—	—	—	—	—	—	—
A6	1.062	428.2	1.064	523.3	—	—	—	—	—	—	0.925	84.2
A7	1.116	380.0	1.082	535.9	—	—	—	—	—	—	1.037	191.9
A8	1.009	450.0	1.062	528.7	—	—	—	—	—	—	0.828	112.2
A9	1.009	454.4	1.060	525.0	—	—	—	—	—	—	0.807	93.4
B1	1.080	553.0	1.014	383.5	—	—	—	—	—	—	—	—
B2	1.101	375.7	1.013	381.8	—	—	—	—	—	—	—	—
B3	0.895	249.2	1.016	383.4	—	—	—	—	—	—	—	—
B4	1.016	274.6	1.014	387.2	—	—	—	—	—	—	—	—
B5	1.153	470.7	1.012	377.9	—	—	—	—	—	—	—	—
B6	1.048	428.7	1.014	384.5	—	—	—	—	—	—	0.935	87.3
B7	1.133	375.4	1.013	373.5	—	—	—	—	—	—	1.032	199.1
B8	1.008	452.4	1.015	388.5	—	—	—	—	—	—	0.827	115.0
B9	1.009	457.9	1.015	386.4	—	—	—	—	—	—	0.806	93.5
C1	1.088	555.4	—	—	1.087	385.8	—	—	—	—	—	—
C2	1.099	375.2	—	—	1.088	355.1	—	—	—	—	—	—
C3	0.908	252.1	—	—	1.101	383.9	—	—	—	—	—	—
C4	1.021	276.2	—	—	1.094	376.6	—	—	—	—	—	—
C5	1.147	467.8	—	—	1.055	341.2	—	—	—	—	—	—
C6	1.050	429.3	—	—	1.080	373.8	—	—	—	—	0.931	72.7
C7	1.119	367.0	—	—	1.055	339.5	—	—	—	—	1.029	168.6
C8	1.014	451.3	—	—	1.083	390.0	—	—	—	—	0.889	106.9
C9	1.015	462.0	—	—	1.090	393.4	—	—	—	—	0.802	85.6
D1	1.082	548.9	—	—	—	—	0.951	282.7	—	—	—	—
D2	1.106	375.2	—	—	—	—	0.970	248.4	—	—	—	—
D3	0.897	172.4	—	—	—	—	0.983	270.4	—	—	—	—
D4	1.018	271.5	—	—	—	—	0.976	267.2	—	—	—	—
D5	1.152	470.9	—	—	—	—	0.960	226.7	—	—	—	—
D6	1.056	428.4	—	—	—	—	0.951	264.2	—	—	0.924	78.8
D7	1.131	374.0	—	—	—	—	0.942	228.7	—	—	1.031	185.7
D8	1.009	447.8	—	—	—	—	0.952	287.7	—	—	0.826	110.9
D9	1.010	452.1	—	—	—	—	0.959	289.1	—	—	0.804	92.9
E1	1.081	552.9	0.985	230.0	—	—	—	—	—	—	—	—
E2	1.104	365.9	0.985	216.0	—	—	—	—	—	—	—	—
E3	0.898	252.2	1.005	236.3	—	—	—	—	—	—	—	—
E4	1.015	276.9	1.005	229.6	—	—	—	—	—	—	—	—
E5	1.147	468.1	1.005	220.5	—	—	—	—	—	—	—	—
E6	1.048	426.6	1.004	233.6	—	—	—	—	—	—	0.937	85.8
E7	1.134	370.7	0.984	212.5	—	—	—	—	—	—	1.035	193.4
E8	1.009	450.1	0.985	233.0	—	—	—	—	—	—	0.827	114.8
E9	1.010	4605	0.995	236.0	—	—	—	—	—	—	0.806	93.4
F1	1.085	554.6	1.116	519.2	—	—	—	—	—	—	—	—
F2	1.106	478.2	1.123	623.1	—	—	—	—	—	—	—	—
F3	0.900	250.4	1.116	516.8	—	—	—	—	—	—	—	—
F4	1.020	276.8	1.116	521.3	—	—	—	—	—	—	—	—
F5	1.160	472.0	1.127	521.8	—	—	—	—	—	—	—	—
F6	1.055	428.7	1.115	517.2	—	—	—	—	—	—	0.932	76.0
F7	1.152	375.8	1.141	525.5	—	—	—	—	—	—	1.038	181.1
F8	1.011	451.8	1.114	521.0	—	—	—	—	—	—	0.825	107.2
F9	1.012	457.7	1.121	519.9	—	—	—	—	—	—	0.804	85.0
G1	1.091	543.0	—	—	1.148	350.0	—	—	1.003	129.1	—	—
G2	1.097	373.3	—	—	1.082	351.1	—	—	1.021	87.8	—	—
G3	0.913	241.2	—	—	1.154	350.8	—	—	1.005	132.9	—	—
G4	1.020	276.9	—	—	1.095	359.6	—	—	1.035	128.5	—	—
G5	1.139	453.4	—	—	1.104	333.6	—	—	0.997	52.9	—	—
G6	1.050	428.2	—	—	1.099	357.6	—	—	1.032	120.7	0.931	69.9

Table 5 (*Contd.*)

Compd.	Ring-R		C–C (bridge)		C–N (bridge)		C–O (bridge)		N–N/N=N (bridge)		$NH–NH_2$/$NH–NO_2$/$C–NO_2$	
	BO	BDE	BO	BDE	BO	BDE	BO	BDE	BO	BDE	BO	BDE
G7	1.128	348.7	—	—	1.091	330.1	—	—	0.957	26.3	1.029	154.6
G8	1.016	428.0	—	—	1.120	335.9	—	—	0.982	101.3	0.821	80.2
G9	1.018	462.6	—	—	1.110	364.9	—	—	1.030	149.5	0.801	83.6
H1	1.084	550.5	—	—	1.136	295.6	—	—	1.720	211.9	—	—
H2	1.119	380.6	—	—	1.124	263.9	—	—	1.767	78.5	—	—
H3	0.890	241.4	—	—	1.156	301.5	—	—	1.709	143.6	—	—
H4	1.024	352.2	—	—	1.137	379.5	—	—	1.703	216.8	—	—
H5	1.196	478.7	—	—	1.207	322.6	—	—	1.616	94.4	—	—
H6	1.071	428.3	—	—	1.145	297.3	—	—	1.706	107.9	0.924	71.1
H7	1.188	384.2	—	—	1.218	327.1	—	—	1.599	76.2	1.041	186.4
H8	1.009	444.7	—	—	1.155	306.6	—	—	1.706	198.1	0.828	96.2
H9	1.008	449.0	—	—	1.152	303.8	—	—	1.714	194.9	0.807	85.2

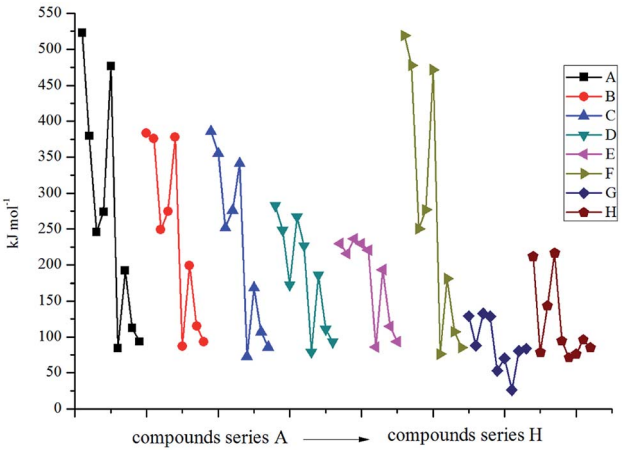

Fig. 4 The variation trends of BDE of the designed compounds.

BDE (69.9 kJ mol^{-1}). The bond order and BDEs of all the designed compounds are summarized and listed in Table 5.

Fig. 4 displays the variation trends of BDEs of the designed compounds. It is seen that the variation trends of BDEs for each series are approximately the same with each other. Incorporating the bridge –CH=CH– (series F) makes less change to the values of BDEs compared to the directly linked ones (series A). For example, the BDEs of compounds A1 and F1 are 522.8 and 519.2 kJ mol^{-1}, and the same is true for compounds A3–A6 and F3–F6. The volatilities of BDEs for each series can be written in the following order: directly linked ≈ –CH=CH– > –C– ≈ –N– > –O– > $–CH_2–CH_2–$ ≈ –N=N– > –NH–NH–. It reveals that the energetic groups acted as the main influence factor on BDEs for the directly linked and –CH=CH– bridged compounds while the parent structure was the most important influence factor for the –NH–NH– bridged ones. The average BDEs of the –NH–NH– bridged ones were found to be the lowest, and, hence, it can be inferred that the introduction of the –NH–NH– bridge might decrease the thermal stability of the 2,2-bi(1,3,4-oxadiazole) derivatives. Evident regularity was also found in each series: BDEs of the –CN, $–N_3$, $–NO_2$, $–NF_2$, $–NH_2$ substituted ones in series A, B, C, E and F were higher than those of the $–NHNO_2$, $–NHNH_2$, $–CH(NO_2)_2$ and $–C(NO_2)_3$ substituted ones. In view of the influence of energetic groups, –CN was the most effective group in improving the BDEs of an energetic material while the $–NHNH_2$ group acted on the opposite side.

It is well known that a promising high-energy-density material should not only have superior detonation properties to those of RDX or HMX, but should also possess acceptable thermal stability. Taking both detonation properties and thermal stabilities[31] into consideration, 22 compounds (A4, A6, A8, A9, B4, B9, C2, C3, C4, C5, C7, C8, C9 D4, D8, D9, E9, F4, F9, G9, H4 and H9) were finally screened as candidates for high-energy explosives with acceptable thermal stabilities.

3.5 Thermodynamic properties

As the main thermodynamic parameters, standard molar heat capacity ($C^{\theta}_{p,m}$) standard molar entropy (S^{θ}_{m}) and standard molar enthalpy (H^{θ}_{m}) can provide useful information on the state equation, macroscopic properties and chemical reactions of an energetic material.[32] The variation trends of $C^{\theta}_{p,m}$, S^{θ}_{m} and H^{θ}_{m} of the title compounds at different temperatures (from 200 to 600 K) were investigated. The related equation for these parameters at different temperatures can be written in the following form:

$$X = a + bT + cT^2 \ (X = C^{\theta}_{p,m},\ S^{\theta}_{m} \text{ and } H^{\theta}_{m})$$

where a, b and c are constants and are summarized in Table 6. It is seen that $C^{\theta}_{p,m}$, S^{θ}_{m} and H^{θ}_{m} of all the designed compounds improved as the temperature increased. However, there existed differences in the growth rates of these parameters. The case is that the growth rates $C^{\theta}_{p,m}$ and S^{θ}_{m} decreased evidently as the temperature increased while the growth rate H^{θ}_{m} increased. The reason is that the translations and rotations of chemical bonds were the main influencing factors at a low temperature while vibrational movement occurred and intensified at a high temperature. At certain temperatures, it was also found that the values of these thermodynamic parameters increases as the

Table 6 Calculated S_m^θ, $C_{p,m}^\theta$ and H_m^θ of the designed compounds

	S_m^θ			$C_{p,m}^\theta$			H_m^θ			
	a	b	$C \times 10^{-4}$	a	b	$C \times 10^{-4}$	a	b	$C \times 10^{-4}$	R^2
A1	250.8	0.70	−2.49	24.3	0.56	−3.22	−4.66	0.07	1.51	0.9999
A2	265.5	0.80	−2.88	29.0	0.64	−3.65	−5.35	0.08	1.73	0.9999
A3	277.4	0.78	−2.65	28.2	0.62	−3.32	−4.11	0.08	1.80	0.9999
A4	274.9	0.84	−2.97	25.0	0.70	−4.16	−5.50	0.09	1.83	0.9999
A5	230.3	0.67	−2.04	10.3	0.61	−3.34	−4.28	0.06	1.70	0.9999
A6	287.4	0.92	−2.96	24.9	0.78	−4.21	−4.90	0.09	2.24	0.9999
A7	252.4	0.81	−2.52	24.0	0.68	−3.30	−4.50	0.07	2.07	0.9999
A8	340.6	1.27	−4.40	54.2	0.97	−4.99	−6.88	0.13	2.86	0.9999
A9	338.7	1.65	−6.39	83.2	1.19	−6.74	−12.8	0.18	3.25	0.9999
B1	267.2	0.77	−2.53	23.8	0.63	−3.37	−4.26	0.07	1.83	0.9999
B2	283.3	0.87	−2.89	27.3	0.72	−3.85	−4.91	0.08	2.06	0.9999
B3	293.5	0.85	−2.66	26.28	0.70	−3.53	−3.77	0.07	2.12	0.9999
B4	290.1	0.90	−2.99	23.07	0.78	−4.38	−5.18	0.09	2.15	0.9999
B5	247.6	0.73	−2.00	7.56	0.69	−3.53	−3.80	0.06	2.04	0.9999
B6	302.5	0.99	−2.98	24.2	0.86	−4.35	−4.51	0.09	2.56	0.9999
B7	269.8	0.87	−2.46	22.0	0.75	−3.47	−3.82	0.07	2.41	0.9999
B8	352.7	1.34	−4.44	53.9	1.04	−5.14	−6.64	0.13	3.18	0.9999
B9	355.7	1.73	−6.43	82.8	1.26	−6.90	−12.5	0.18	3.57	0.9999
C1	260.4	0.78	−2.76	24.9	0.64	−3.70	−5.40	0.08	1.70	0.9999
C2	285.4	0.89	−3.20	31.3	0.71	−4.10	−5.98	0.09	1.92	0.9999
C3	285.3	0.86	−2.89	28.1	0.70	−3.79	−4.82	0.08	2.00	0.9999
C4	294.5	0.92	−3.26	26.0	0.78	−4.65	−6.10	0.09	2.02	0.9999
C5	245.5	0.74	−2.29	12.2	0.68	−3.72	−4.80	0.06	1.89	0.9999
C6	296.0	1.00	−3.26	26.2	0.86	−4.69	−5.76	0.09	2.43	0.9999
C7	267.7	0.89	−2.73	24.2	0.76	−3.78	−4.92	0.08	2.28	0.9999
C8	348.5	1.35	−4.70	55.5	1.04	−5.46	−7.72	0.13	3.05	0.9999
C9	345.5	1.74	−6.67	84.0	1.27	−7.22	−13.6	0.19	3.44	0.9999
D1	264.3	0.75	−2.70	24.5	0.61	−3.60	−5.03	0.08	1.62	0.9999
D2	283.6	0.86	−3.11	28.7	0.70	−4.12	−5.76	0.09	1.85	0.9999
D3	276.9	0.80	−2.61	21.0	0.68	−3.74	−4.52	0.08	1.91	0.9999
D4	286.8	0.90	−3.20	24.5	0.76	−4.63	−6.03	0.09	1.95	0.9999
D5	249.5	0.72	−2.21	9.11	0.67	−3.77	−4.53	0.06	1.83	0.9999
D6	298.8	0.98	−3.17	24.9	0.84	−4.61	−5.35	0.09	2.36	0.9999
D7	267.2	0.86	−2.62	21.7	0.74	−3.75	−4.59	0.08	2.21	0.9999
D8	352.1	1.32	−4.61	54.7	1.02	−5.38	−7.34	0.13	2.98	0.9999
D9	355.4	1.71	−6.62	84.05	1.24	−7.12	−13.2	0.19	3.36	0.9999
E1	282.1	0.84	−2.57	23.9	0.71	−3.50	−3.83	0.07	2.14	0.9999
E2	295.8	0.94	−2.97	28.8	0.79	−3.94	−4.61	0.09	2.37	0.9999
E3	307.1	0.92	−2.77	30.2	0.76	−3.53	−3.36	0.08	2.43	0.9999
E4	300.7	0.98	−3.05	23.1	0.85	−4.55	−5.08	0.09	2.47	0.9999
E5	263.0	0.80	−2.12	12.3	0.74	−3.49	−3.39	0.06	2.33	0.9999
E6	311.6	1.05	−3.00	23.2	0.93	−4.51	−4.36	0.09	2.88	0.9999
E7	282.6	0.94	−2.52	22.0	0.83	−3.64	−3.55	0.07	2.72	0.9999
E8	371.3	1.41	−4.48	54.1	1.11	−5.27	−6.18	0.13	3.50	0.9999
E9	369.1	1.80	−6.50	84.0	1.33	−7.00	−12.2	0.19	3.88	0.9999
F1	265.8	0.82	−2.74	25.7	0.68	−3.67	−4.92	0.07	1.94	0.9999
F2	281.5	0.93	−3.14	30.9	0.76	−4.10	−5.62	0.09	2.17	0.9999
F3	289.5	0.90	−2.88	28.3	0.75	−3.83	−4.51	0.08	2.24	0.9999
F4	291.4	0.97	−3.24	26.7	0.82	−4.63	−5.80	0.09	2.26	0.9999
F5	246.4	0.79	−2.27	11.4	0.73	−3.79	−4.65	0.07	2.14	0.9999
F6	301.6	1.04	−3.19	25.0	0.91	−4.71	−5.23	0.09	2.68	0.9999
F7	265.8	0.93	−2.71	22.8	0.81	−3.90	−4.85	0.08	2.52	0.9999
F8	356.6	1.39	−4.66	56.1	1.09	−5.44	−7.15	0.13	3.30	0.9999
F9	355.6	1.78	−6.63	82.7	1.32	−7.29	−13.1	0.19	3.69	0.9999
G1	249.6	0.82	−2.75	19.9	0.70	−4.05	−6.02	0.08	1.89	0.9999
G2	285.2	0.95	−3.30	28.8	0.79	−4.50	−6.36	0.10	2.15	0.9999
G3	270.6	0.90	−2.93	24.6	0.77	−4.13	−5.63	0.09	2.18	0.9999
G4	288.2	1.00	−3.51	27.2	0.85	−5.07	−7.06	0.10	2.22	0.9999
G5	236.0	0.77	−2.16	4.67	0.74	−4.03	−5.00	0.06	2.11	0.9999
G6	293.5	1.08	−3.46	26.0	0.93	−5.10	−6.38	0.10	2.64	0.9999
G7	257.5	0.89	−2.42	11.3	0.83	−4.15	−4.67	0.07	2.53	0.9999

Table 6 (*Contd.*)

	S^{θ}_{m}			$C^{\theta}_{p,m}$			H^{θ}_{m}			
	a	*b*	$C \times 10^{-4}$	*a*	*b*	$C \times 10^{-4}$	*a*	*b*	$C \times 10^{-4}$	R^2
G8	339.0	1.37	−4.54	47.2	1.11	−5.79	−7.75	0.13	3.28	0.9999
G9	356.1	1.81	−6.88	84.6	1.34	−7.61	−14.2	0.20	3.65	0.9999
H1	270.7	0.81	−2.96	31.4	0.64	−3.64	−5.46	0.09	1.73	0.9999
H2	280.6	0.91	−3.26	31.1	0.74	−4.27	−6.23	0.09	1.98	0.9999
H3	291.0	0.89	−3.06	31.0	0.72	−3.92	−5.10	0.09	2.04	0.9999
H4	289.1	0.95	−3.41	29.5	0.79	−4.71	−6.54	0.10	2.06	0.9999
H5	238.8	0.78	−2.47	13.8	0.70	−3.94	−5.68	0.07	1.93	0.9999
H6	303.1	1.04	−3.43	31.7	0.86	−4.65	−5.80	0.09	2.46	0.9999
H7	267.8	0.93	−3.00	31.1	0.76	−3.82	−5.48	0.09	2.30	0.9999
H8	345.5	1.38	−4.79	56.7	1.06	−5.60	−8.01	0.14	3.10	0.9999
H9	350.4	1.77	−6.80	86.2	1.28	−7.34	−13.8	0.20	3.48	0.9999

volume of energetic groups increased. This phenomenon may be caused by the strong space steric effects of the energetic groups. Take compounds A8 and A9 for example, $C^{\theta}_{p,m}$, S^{θ}_{m} and H^{θ}_{m} of compound A8 and A9 were 228.2 kJ mol^{-1} K^{-1}, 575.8 kJ mol^{-1} K^{-1}, 30.1 kJ mol^{-1} and 294.0 kJ mol^{-1} K^{-1}, 643.5 kJ mol^{-1} K^{-1}, 37.1 kJ mol^{-1}, respectively (200 K). Obviously, $C^{\theta}_{p,m}$, S^{θ}_{m} and H^{θ}_{m} of compound A9 were higher than those of compound A8.

4. Conclusions

In this study, a series of bridged 2,2-bi(1,3,4-oxadiazole) energetic derivatives were designed and investigated by the density functional theory method at B3LYP/6-311G(d,p) level. The substitution of –CH_2–, –O– and –CH_2–CH_2– bridges improves the HOMO–LUMO gap while the –N=N– bridge decreases the values. Most of the designed compounds (except for B5, D4, D5, E4, E5 and F5) possess high positive heats of formation (range from 15.4 to 1148.6 kJ mol^{-1}). The –N_3 and –NH– groups act as effective structural units for increasing the solid-phase heats of formation of these derivatives. The calculated detonation properties show that the –NF_2 and –NH– groups can improve the heats of detonation, detonation velocities and detonation pressures evidently. The analysis of the bond dissociation energies suggests that most of the designed compounds have acceptable thermal stabilities with the values ranging from 26.3 to 522.8 kJ mol^{-1}. Finally, 22 compounds (A4, A6, A8, A9, B4, B9, C2, C3, C4, C5, C7, C8, C9 D4, D8, D9, E9, F4, F9, G9, H4 and H9) were selected as potential candidates for promising high-energy-density materials.

Conflicts of interest

There are no conflicts to declare.

Acknowledgements

This study was supported by the National Natural Science Foundation of China (Grant No. 11602121).

References

1 C. Zhang, C. G. Sun, B. C. Hu, C. M. Yu and M. Lu, *Science*, 2017, **355**, 374–376.
2 M. B. Talawar, R. Sivabalan, T. Mukundan, H. Muthurajan, A. K. Sikder, B. R. Gandhe and A. S. Rao, *J. Hazard. Mater.*, 2009, **161**, 589–607.
3 V. D. Ghule, D. Sonal, A. Devi and T. R. Kumar, *Ind. Eng. Chem. Res.*, 2016, **55**, 875–881.
4 A. K. Sikder and N. Sikder, *J. Hazard. Mater.*, 2004, **112**, 1–15.
5 X. H. Jin, J. H. Zhou, S. J. Wang and B. C. Hu, *Quim. Nova*, 2016, **39**, 467–473.
6 W. Chi, *RSC Adv.*, 2015, **5**, 7766–7772.
7 W. Chi, L. L. Li, B. T. Li and H. S. Wu, *Struct. Chem.*, 2012, **23**, 1837–1841.
8 Z. Fu, R. Su, Y. Wang, Y. F. Wang, W. Zeng, N. Xiao, Y. Wu, Z. Zhou, J. Chen and F. Chen, *Chem.– Eur. J.*, 2012, **18**, 1886–1889.
9 A. V. Sergievskii, T. V. Romanova, S. F. Melikova and I. V. Yselinskii, *Russ. J. Org. Chem.*, 2005, **41**, 261–267.
10 J. H. Zhang and J. M. Shreeve, *J. Am. Chem. Soc.*, 2014, **136**, 4437–4445.
11 H. Wei, C. L. He, J. H. Zhang and J. M. Shreeve, *Angew. Chem., Int. Ed.*, 2015, **54**, 9367–9371.
12 J. A. Joule, K. Mills and G. F. Smith, *Heterocyclic Chemistry*, Taylor & Francis, New York, 3rd edn, 1995.
13 W. Q. Zhang, J. H. Zhang, M. C. Deng, X. J. Qi, F. D. Nie and Q. H. Zhang, *Nat. Commun.*, 2017, **8**, 181–187.
14 Q. Wu, W. H. Zhu and H. M. Xiao, *J. Chem. Eng. Data*, 2013, **58**, 2748–2762.
15 F. Wang, G. X. Wang, H. C. Du, J. Y. Zhang and X. D. Gong, *J. Phys. Chem. A*, 2011, **115**, 13858–13864.
16 M. J. Frisch, G. W. Trucks, H. B. Schlegel, G. E. Scuseria, M. A. Robb, J. R. Cheeseman, J. A. Montgomery, T. Vreven, K. N. Kudin, J. C. Burant, J. M. Millam, S. S. Iyengar, J. Tomasi, V. Barone, B. Mennucci, M. Cossi, G. Scalmani, N. Rega, G. A. Petersson, H. Nakatsuji, M. Hada, M. Ehara, K. Toyota, R. Fukuda, J. Hasegawa, M. Ishida, T. Nakajima, Y. Honda, O. Kitao, H. Nakai, M. Klene, X. Li, J. E. Knox,

H. P. Hratchian, J. B. Cross, C. Adamo, J. Jaramillo, R. Gomperts, R. E. Stratmann, O. Yazyev, A. J. Austin, R. Cammi, C. Pomelli, J. W. Ochterski, P. Y. Ayala, K. Morokuma, G. A. Voth, P. Salvador, J. J. Dannenberg, V. G. Zakrzewski, S. Dapprich, A. D. Daniels, M. C. Strain, O. Farkas, D. K. Malick, A. D. Rabuck, K. Raghavachari, J. B. Foresman, J. V. Ortiz, Q. Cui, A. G. Baboul, S. Clifford, J. Cioslowski, B. B. Stefanov, G. Liu, A. Liashenko, P. Piskorz, I. Komaromi, R. L. Martin, D. J. Fox, T. Keith, M. A. Al-Laham, C. Y. Peng, A. Nanayakkara, M. Challacombe, P. M. W. Gill, B. Johnson, W. Chen, M. W. Wong, C. Gonzalez and J. A. Pople, *Gaussian 03*, Gaussian Inc, Pittsburgh, PA, 2003.

17 Y. H. Joo, B. Twamley, S. Garg and J. M. Shreeve, *Angew. Chem., Int. Ed.*, 2008, **120**, 6332–6335.

18 Y. Y. Guo, W. J. Chi, Z. S. Li and Q. S. Li, *RSC Adv.*, 2015, **5**, 38048–38055.

19 X. H. Jin, J. H. Zhou, B. C. Hu and C. M. Ma, *J. Phys. Org. Chem.*, 2017, **30**, e3704.

20 G. H. Tao, B. Twamley and J. M. Shreeve, *J. Mater. Chem.*, 2009, **19**, 5850–5854.

21 K. E. Gutowski, R. D. Rogers and D. A. Dixon, *J. Phys. Chem. B*, 2007, **111**, 4788–4800.

22 B. S. Jursic, *J. Mol. Struct.: THEOCHEM*, 2000, **499**, 137–140.

23 P. W. Atkins, *Physical Chemistry*. Oxford University Press, Oxford, 2nd edn, 1982.

24 P. Politzer, Y. Ma, P. Lane and M. C. Concha, *Int. J. Quantum Chem.*, 2005, **105**, 341–347.

25 E. F. C. Byrd and B. M. Rice, *J. Phys. Chem. A*, 2006, **110**, 1005–1013.

26 P. Politzer, J. Martinez, J. S. Murray, M. C. Concha and A. Toro-Labbé, *Mol. Phys.*, 2009, **107**, 2095–2101.

27 M. J. Kamlet and S. J. Jacobs, *J. Chem. Phys.*, 1968, **48**, 23–25.

28 D. H. Ess and K. N. Houk, *J. Am. Chem. Soc.*, 2008, **130**, 10187–10198.

29 B. M. Rice, S. V. Pai and J. Hare, *Combust. Flame*, 1999, **118**, 445–458.

30 Y. Pan, W. H. Zhu and H. M. Xiao, *J. Mol. Model.*, 2012, **18**, 3125–3138.

31 G. S. Chung, M. W. Schmidt and M. S. Gordon, *J. Phys. Chem. A*, 2000, **104**, 5647–5650.

32 J. Zhang and H. M. Xiao, *J. Chem. Phys.*, 2002, **116**, 10674–10683.